International Journal of Mechanical Engineering and Technology (IJMET)

Volume 12, Issue 12, December 2021, pp. 19-29. Article ID: IJMET_12_12_003 Available online at https://iaeme.com/Home/issue/IJMET?Volume=12&Issue=12

Available online at https://iaeme.com/Home/issue/IJMET?Volume=12& ISSN Print: 0976-6340 and ISSN Online: 0976-6359

DOI: https://doi.org/10.17605/OSF.IO/E32PV

© IAEME Publication



THE INFLUENCE OF SUBMERGED ARC WELDING CONDITIONS ON THE PROPERTIES OF S355JR STRUCTURAL STEEL JOINTS

Agata Wieczorska^{1*}, Rafał Domżalski²

¹Uniwersytet Morski w Gdyni, Wydział Mechaniczny Ul.Morska 81-87, 81-225 Gdynia, Poland ORCID: 0000-0002-6196-7915

²Metal Expert Sp. z o.o. Sp. J., Ul. Kwiatkowskiego 14, 82-300 Elbląg, Poland *Corresponding Author

ABSTRACT

The article presents the tests performed to determine the operating parameters and welding conditions for the S355JR structural steel using the Submerged Arc Welding (SAW) method. The tests were carried out on samples made of S355JR steel after welding performed in accordance with the PN-EN 15614 standard. The work analyzed the depth of penetration of the welding arc depending on various welding parameters of the tested samples. For the obtained results linear energy was calculated for the given welding parameters.

Keywords: Depth of fusion, Linear energy for welding, Penetration, Structural steel, Submerged Arc Welding (SAW).

Cite this Article: Agata Wieczorska and Rafał Domzalski, The Influence of Submerged Arc Welding Conditions on the Properties of S355JR Structural Steel Joints, *International Journal of Mechanical Engineering and Technology (IJMET)*, 12(12), 2021, pp. 19-29.

https://iaeme.com/Home/issue/IJMET?Volume=12&Issue=12

1. INTRODUCTION

The submerged arc welding (SAW) method is mainly used for welding and surfacing of low-carbon steels, low-alloy steels with increased strength, low-alloy steels for the power industry and high-alloy steels. Submerged arc welding is also used for non-ferrous metals (copper, aluminum, titanium and alloys of these metals) using special fluxes. High currents used during SAW welding allow to weld thicker workpieces and obtain high welding efficiency [1]. The submerged arc welding is used, among others, in in the production of large tanks for the chemical industry, beams and sections as well as hull sections of sea-going ships. The industry also uses stainless steel hard facing of the inner surfaces of carbon steel tanks for the chemical industry.



The article presents the tests performed to determine the operating parameters and welding conditions for the S355JR structural steel using the SAW method. Samples made of S355JR structural steel were tested. The elements from which the samples were made were welded in accordance with the PN-EN 15614 standard. Before welding, the welded elements were properly prepared. The edges of the welded elements have been cleaned.

The commencement of the welding process consists in [9]:

- setting the path of the welding head movement parallel to the weld line with the beginning of the electrode in the place of the run-out plates,
- opening the flux charge so that it fills the initial space of the welding groove,
- parameter setting,
- process inclusion.

Electrode feeding and head movement will start. The arc ignites under the flux charge and is invisible. During welding, the operator should check that the electrode is always in the axis of the welding groove and, if necessary, correct the direction of the head movement. The control during welding is carried out on the basis of the indications of instruments displaying welding parameters and the electrode position indicator [2,3,4]

In submerged arc welding, the shape and dimensions of the welds depend on:

- current parameters (U and I),
- welding speed,
- electrode diameter,
- type of current,
- polarity,
- inclination of the electrode in relation to the weld,
- the shape of the bevelled edges [8,9].

Momentary instability occurs when starting and stopping welding process, so that the weld in these places does not have the required properties.

To maintain the homogeneity of the joint along the entire length of the joint, run-out plates are used at the beginning and at the end of the joint, which are cut off after welding (Figure 1).

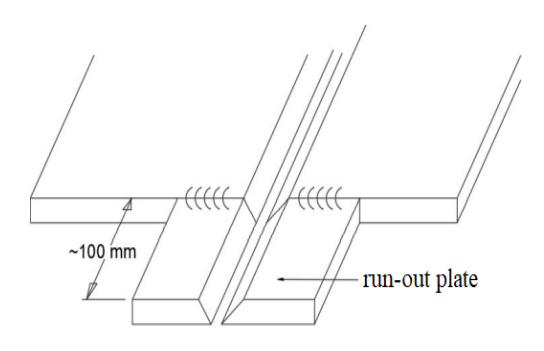


Figure 1 The drawing shows the prepared joint with the run-out plate [1]

In order to weld at higher speeds and obtain higher efficiency, in one-sided welding, special technological washers are used - their task is to eliminate the leakage of the weld metal from the weld groove and form an even and correct root. Backing plates for submerged arc welding are necessary because the arc energies are much higher (greater volume of liquid metal) than for MMA welding [5,6,7].

2. EXPERIMENTAL

The sample consisted of two plates with dimensions of 40x100x1300, one of which was chamfered to the dimensions given in the drawing below (Figure 2). Additionally, a spacer was used - a plate with dimensions of 6x200x1300. The plate was divided into 4 main sections (sections 1-4), which were separated by intermediate sections. The plate had a run-up and an exit section, the last 50mm of which was left without a weld in order to be cut off later as a joint template.

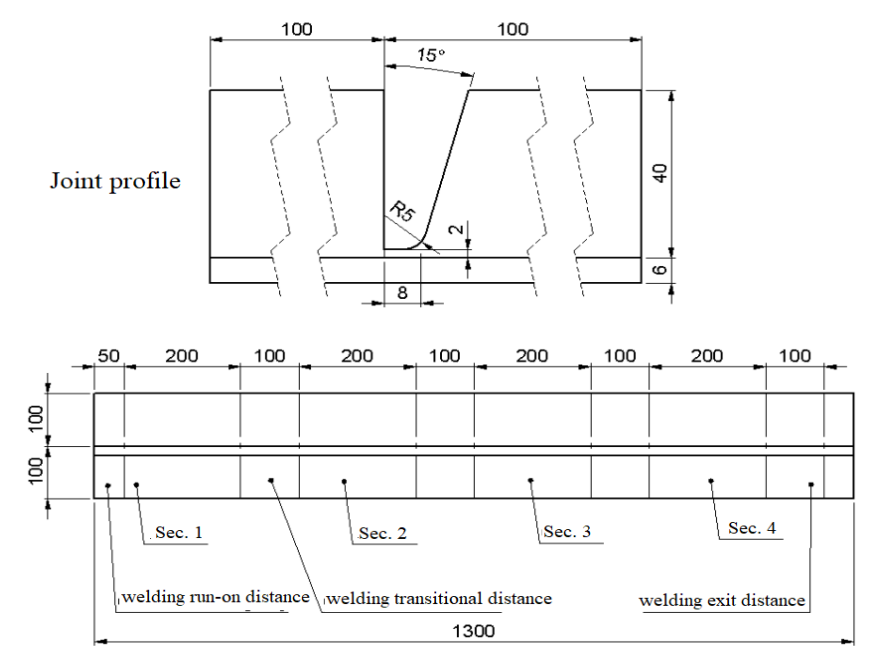


Figure 2. Geometry of sample.

Table 1 presents the material data and welding parameters.

Welding process	121 (SAW)
Joint type	BW
Welding position	PA
Base material	S355JR
Dimension of testing plates	2x40x100x1300
Filler material	Ø4, BA-S3Si
Flux	BF 10 SA FB 155AC
Preheat temperature	100-150°C

Table 1 Material data and welding parameters

The welding parameters for individual sections are summarized in Table 2.

Table 2 Welding parameters for individual sections of sampleSectionArc Voltage UWeldingWelding

Section	Arc Voltage U [V]	Welding Current I [A]	Welding speed [cm/min]
1	30	680	42
2	30	610	35
3	30	540	49
4	30	600	60

The sample was welded continuously through all test sections, i.e. without switching the process off and on, and the parameters were changed during the head's run in transition zone.

Each bead of welding was led along a straight wall, and the distance of the welding wire from the wall was successively:

- bead of welding 1 2 mm
- bead of welding 2-3-3 mm
- bead of welding 4-n-4 mm

In the Figure 3 the sample during welding is presented.

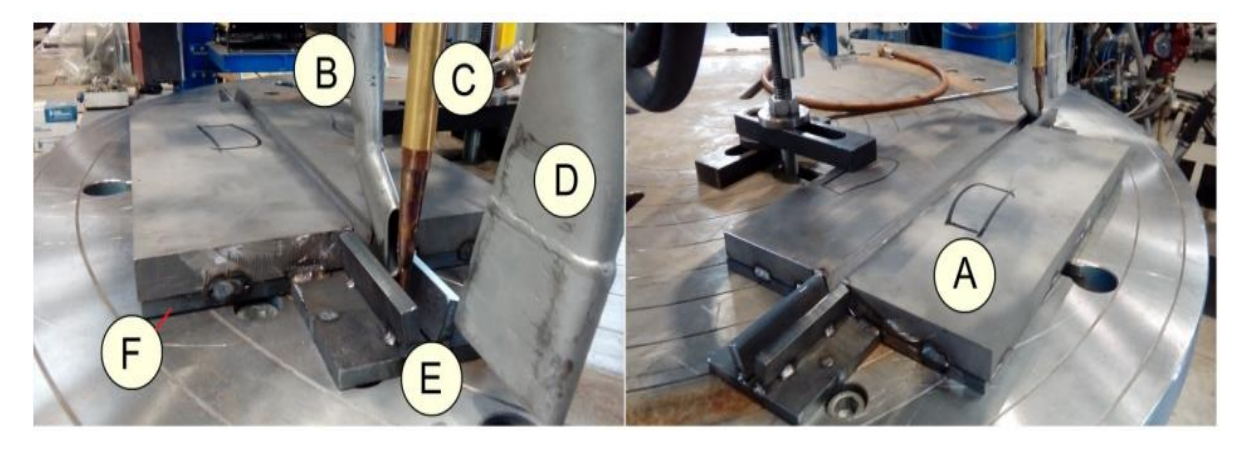


Figure 3. Sample S355JR, 40 mm thick: A. Sample 1/2V, 15 ° bevel, B. Flux charge, C. Current nozzle, D. Suction of flux surplus, E. Run-out plates, F. Washer

From each welded section, 3 samples with dimensions of 10x46x200 were taken as shown in Figure 4. They were appropriately marked depending on the section from which they were taken:

Section I:

- 681
- 682
- 683

Section II:

- 611
- 612
- 633

Section III:

- 541
- 542
- 543

Section IV:

- 601
- 602
- 603

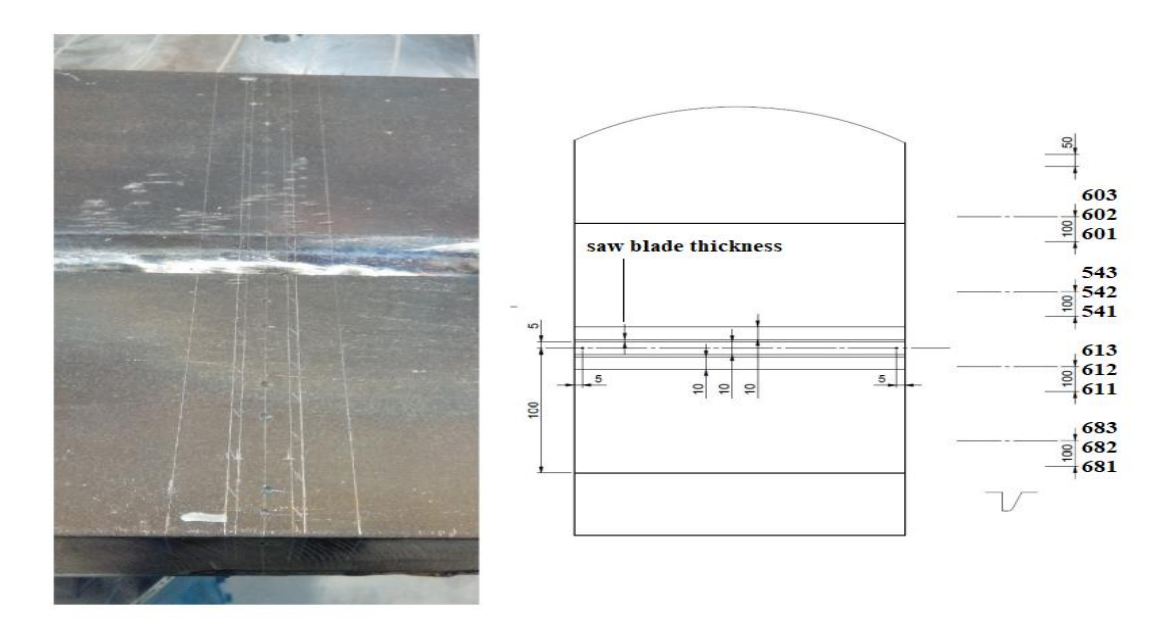


Figure 4. The method of tracing the cutting line of samples from the tested joint

After etching the macroscopic specimens, photos of the weld cross-sections were taken, on the basis of which further tests were carried out.

The tests were carried out on twelve cross-sections of the welded joint. The scope of test methods, equipment used and test documents are shown in Table 3. Defects were classified on the basis of PN-EN ISO 6520-1: 2009.

Table 3. Research methods, research equipment, standards

Testing method	Test equipment	Testing specification	Test standards and instructions
Macroscopy	STEMI 2000c	magn. x2+10	PN-EN ISO 1
		etch. Ma23Fe	7639:2013-12

Figures 5, 6, 7, 8 show macroscopic specimens showing the defects along with the type of defect in the joint. Tables 4, 5, 6, 7 describe the type of welding defects with the classification of defects on the basis of PN-EN ISO 6520-1: 2009 and the size of the defect along with its location in the weld.

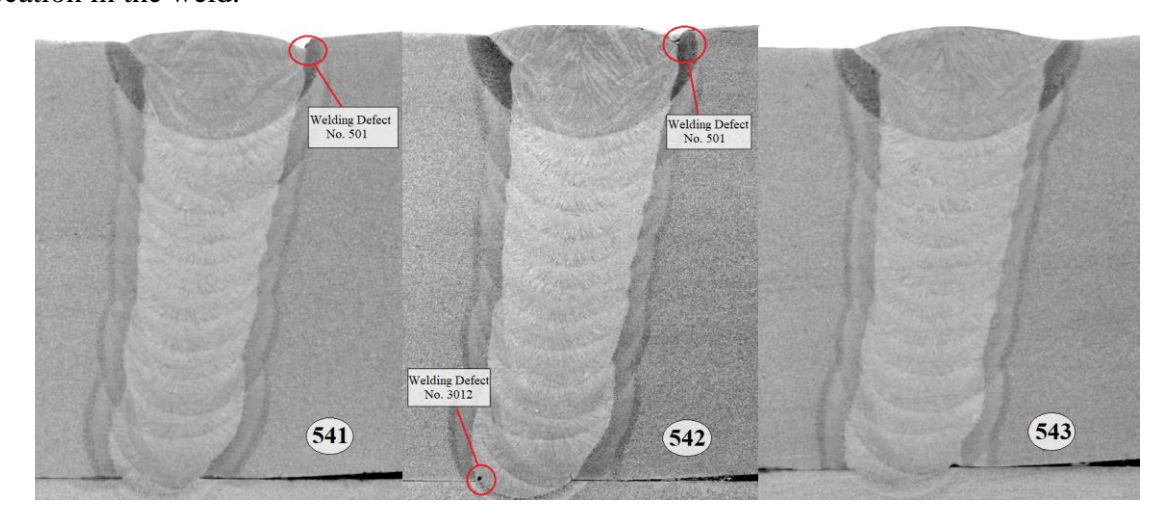


Figure 5 The macrostructure on the cross-section of a welded joint with the following parameters: *No.* 541/542/543 -540 A, 30 V, 49 cm / min.

	77 070		G	
No.	Name of defects	Symbol	Size [mm]	Notes
541/540A	Sealing run	501	1,0 mm	Right side of the weld joint
542/540A	Sealing run	501	1,4 mm	Right side of the weld jont
	Isolated Slag Inclusion	3012	0,6x0,45	Root of weld, left side of the weld jont
543/540A	No defects were found	-	-	-

Table 4. The results of macroscopic testing for samples No. 541,542,543

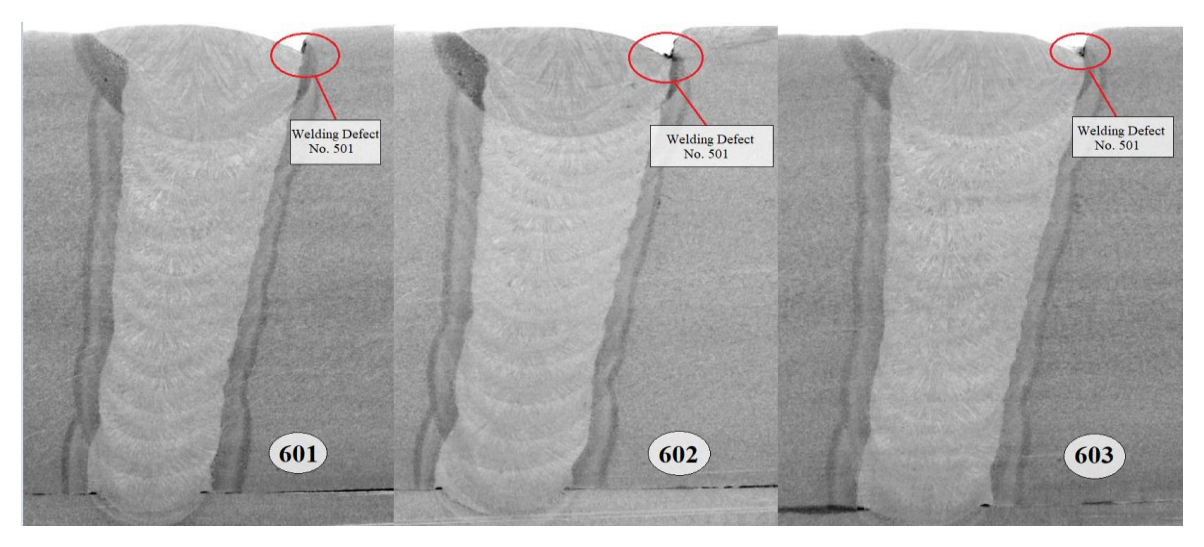


Figure 6. The macrostructure on the cross-section of a welded joint with the following parameters: *No.* 601/602/603 -600 A, 30 V, 60 cm/min.

Table 5 The results of macroscopic testing for samples No. 601,602,603

No.	Name of defects	Symbol	Size [mm]	Notes
601/600A	Sealing run	501	2,1 mm	Right side of the weld jont
602/600A	Sealing run	501	2,8 mm	Right side of the weld jont
603/600A	Sealing run	501	2,4 mm	Right side of the weld jont

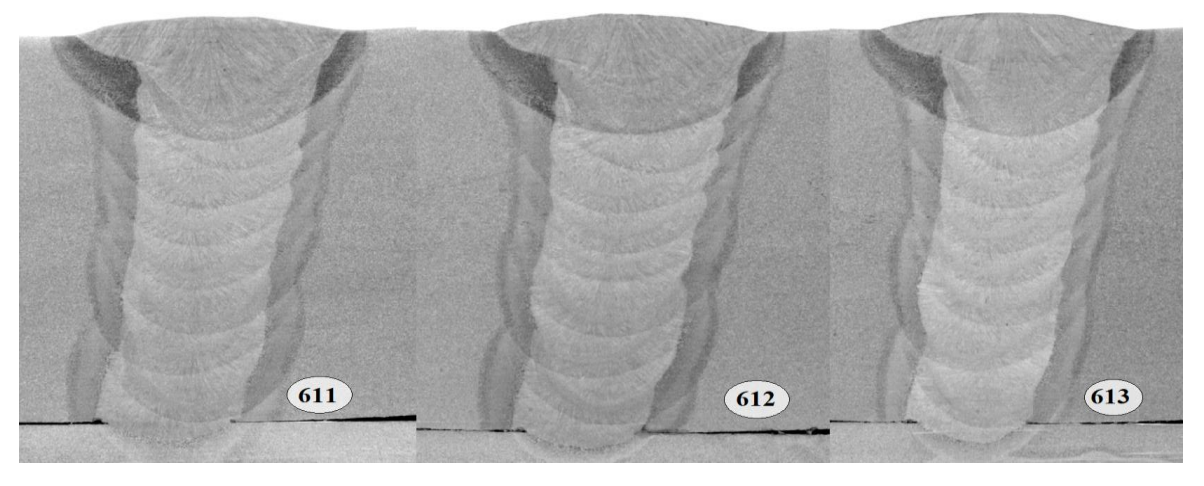


Figure 7. The macrostructure on the cross-section of a welded joint with the following parameters:

No. 611/612/613 -610 A, 30 V, 35 cm / min.

Table 6. The results of macroscopic testing for samples No. 611,612,613

No.	Name of defects	Symbol	Size [mm]	Notes
611/610A	No defects were	-	-	-
	found			
612/610A	No defects were	-	-	
	found			-
L 613/61UA	No defects were	_	_	_
	found	_	_	_

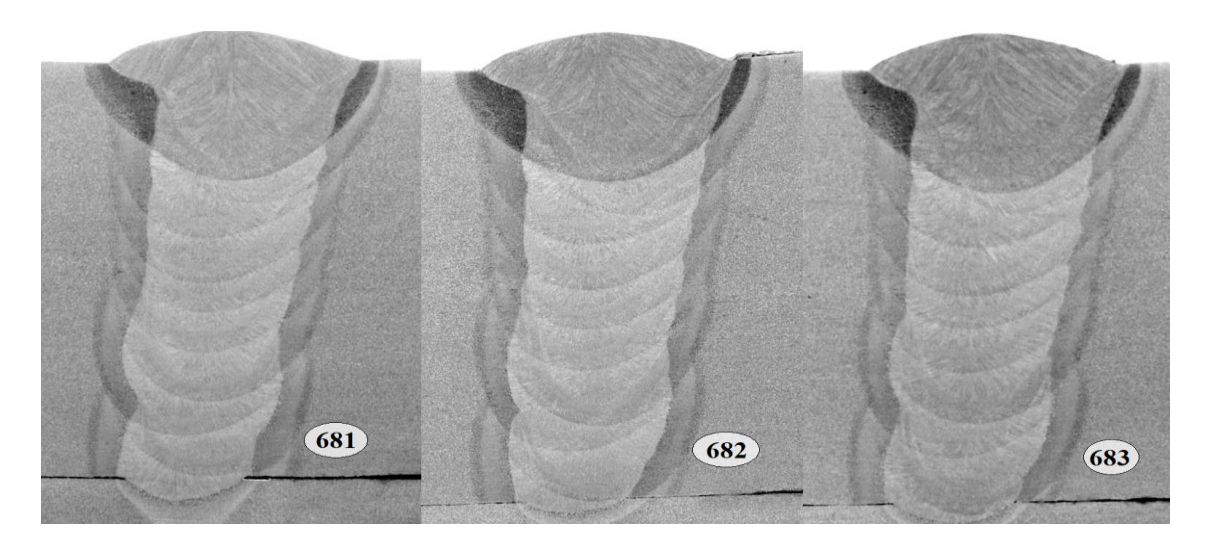


Figure 8. The macrostructure on the cross-section of a welded joint with the following parameters: No. 681/682/683 -680 A, 30 V, 42 cm / min.

Table 7. The results of macroscopic testing for samples No. 681,682,683

No.	Name of defects	Symbol	Size [mm]	Notes
681/680A	No defects were			
061/060A	found	-	-	-
682/680A	No defects were			
	found	-	•	-
$A \times A / A /$	No defects were			
	found	-	-	-

The further part of the research was to determine the depth of fusion of the welding arc depending on the welding parameters. Photographs of macroscopic examinations served this purpose. The depth of fusion penetration of the welding arc was carried out for all samples, the results are summarized in Table 8. Figures 9, 10, 11 show examples of the measurement of the penetration depth for samples no. 541,601,681. The photos show etched metallographic specimens with a sketch of the joint profile and the determined distances of visible penetrations in the native material.

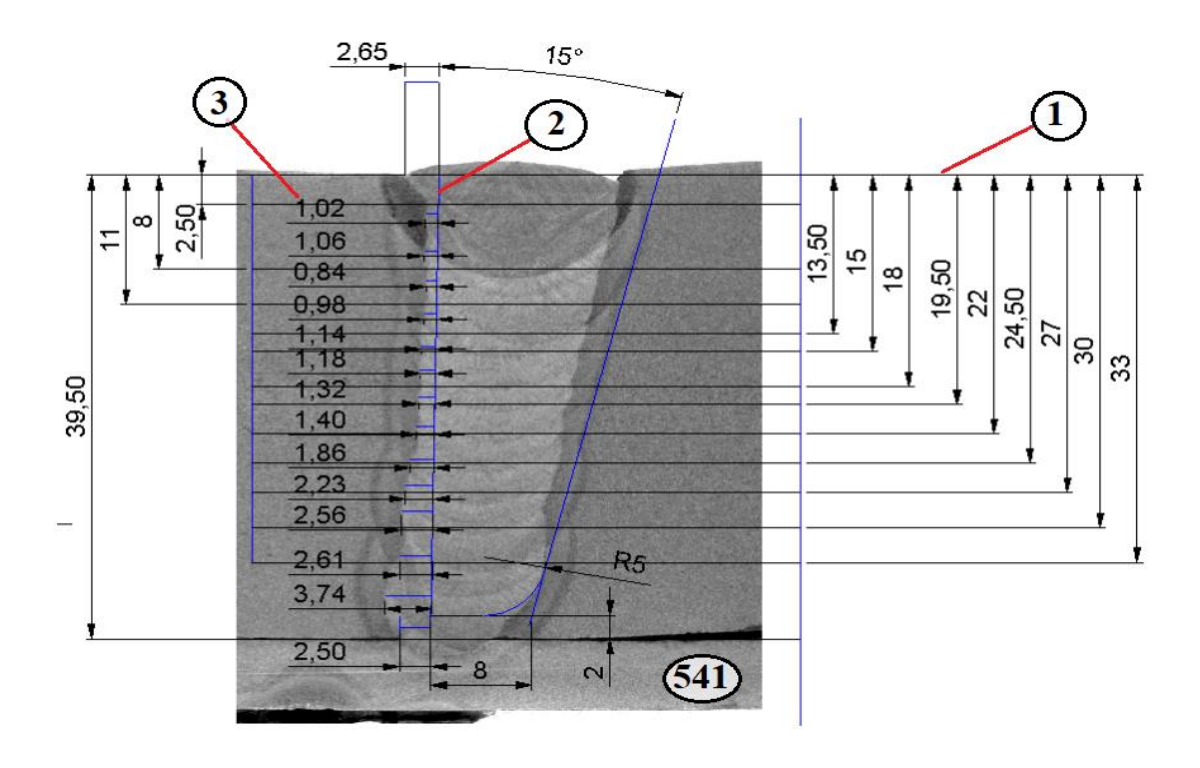


Figure 9. The measurement depth of fusion penetration the welding arc on sample no. 541, 1 – bead heights, 2 - straight wall line, 3 - depth of fusion penetration

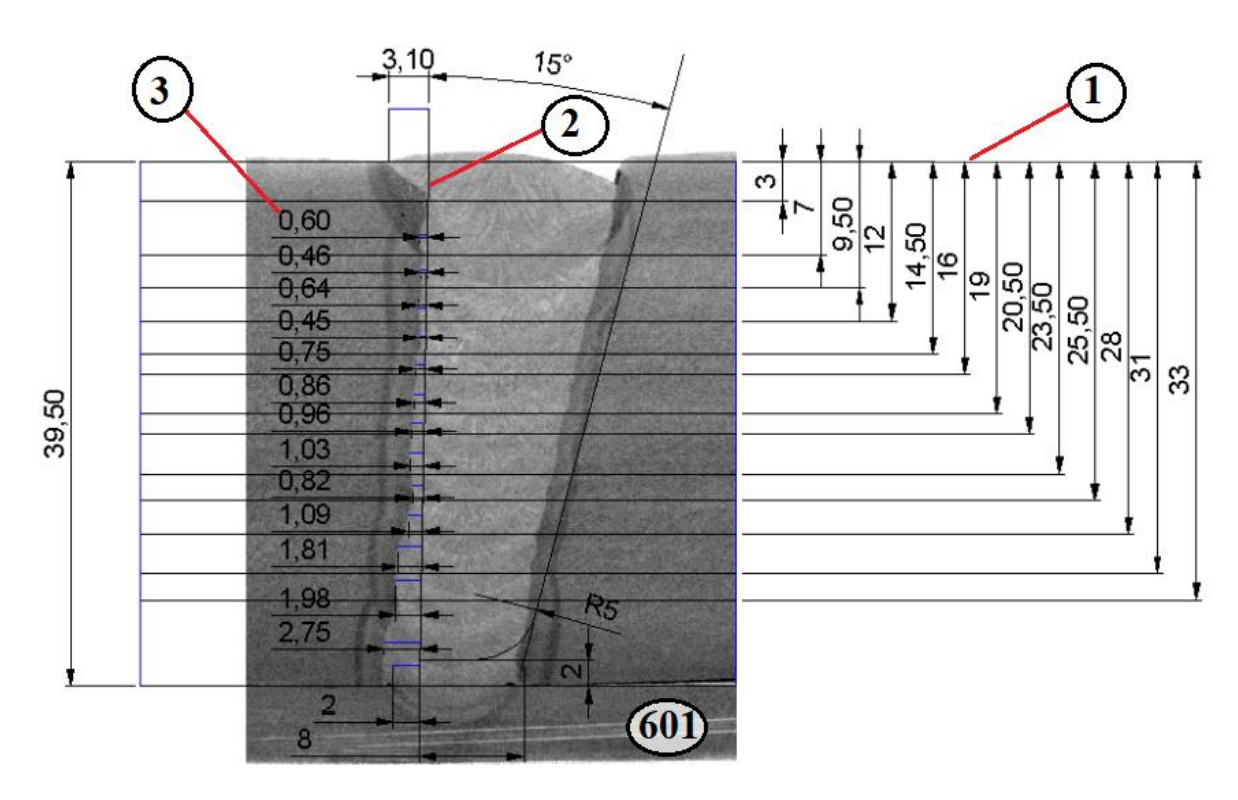


Figure 10. The measurement depth of fusion penetration the welding arc on sample no. 601, 1 – bead heights, 2 - straight wall line, 3 - depth of fusion penetration

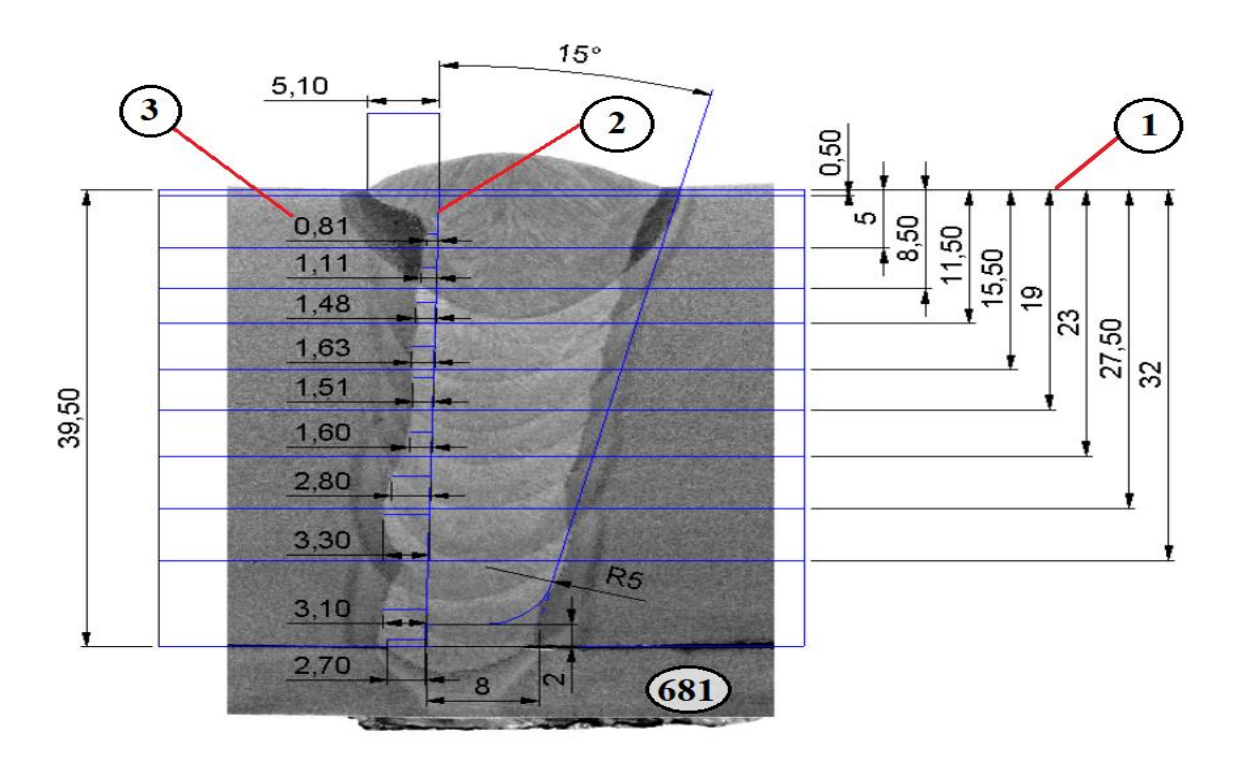


Figure 11 The measurement depth of fusion penetration the welding arc on sample no. 601, 1 – bead heights, 2 - straight wall line, 3 - depth of fusion penetration

3. RESULTS AND DISCUSSION

The results of the depth of fusion penetration test for all samples are presented in the diagram (Fig. 12).

The linear energy for the given welding parameters has been converted according to the formula:

$$Q=k\frac{U\cdot I}{v}\cdot 10^{-3} kJ/mm$$

where:

k-factor for the SAW method = 1.

As you can read from Table 8, most of the heat was introduced into the weld in section 2, then 1., successively 3., and the least in section 4. Unfortunately, this does not coincide with the assumptions, because the penetration depths for section 1 are slightly smaller than for segment 3, and there is a large difference between them in the value of linear energy. I assume that the reason for these results is that the specimen had sufficiently warmed up by the time section 3 was started to be welded.

The penetration depths have shown that even when the welding wire is moved 4 mm away from the wall, a satisfactory penetration can be obtained.

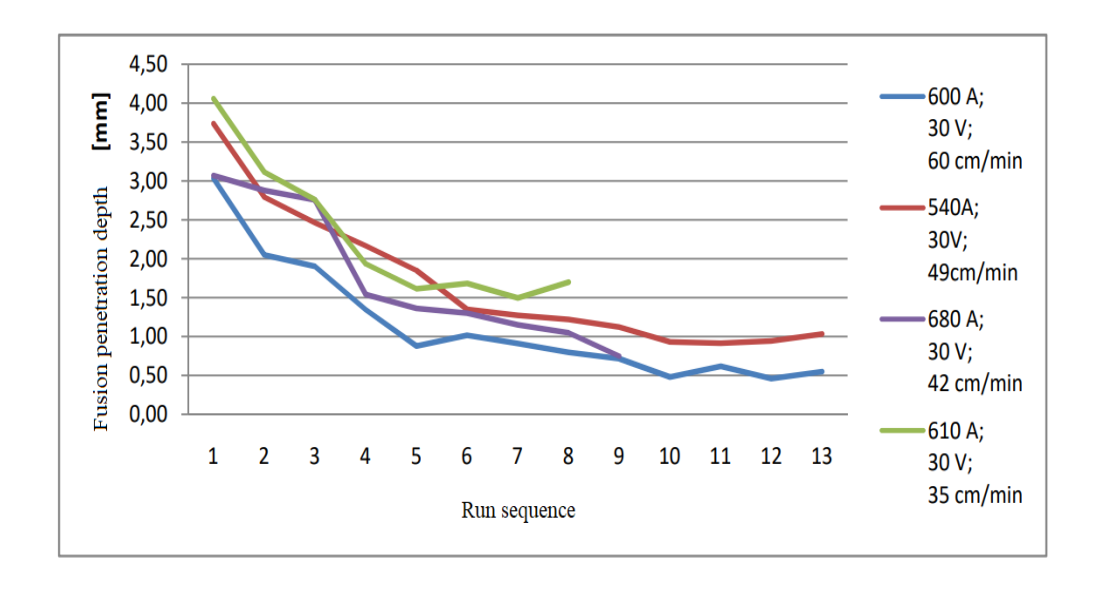


Figure 12 The results depth of fusion penetration depending on the welding parameters

Section	Arc Voltage U [V]	Welding Current I [A]	Welding speed [cm/min]	Linear energy Q[kJ/mm]
1	30	680	42	2,91
2	30	610	35	3,14
3	30	540	49	1,98
4	30	600	60	1,80

Table 8 The linear energies for welding parameters

4. CONCLUSIONS

As a result of the analysis of the test results, it was noticed that carrying out the process at higher speeds results in easier removal of the slag from the welding groove and introduces smaller deformations.

At the same time, it has been observed that running the process at increased speeds requires more stitches, which in turn means a greater number of thermal cycles, which can negatively affect the quality of the joint during service.

As a result of the observation of the tested joints, it was observed that the first of the tested joints contained many defects, such as sticking and slag inclusions inside the joints. Additionally, difficulties arose in obtaining welds with the correct profile and in removing the slag from the weld groove. These obstacles were eliminated by the experimental method by carrying out subsequent tests with the use of various parameters and the geometry of the welding grooves.

REFERENCES

- [1] GawroniakN.: Podstawy spawalnictwa. Wydawnictwo Politechniki Gdańskiej. Gdańsk 2004
- [2] Cecotka M., Wnuk M.:Zastosowanie metody spawania wąskoszczelinowego w energetyce. Przegląd Spawalnictwa 7/2014.
- [3] Pilarczyk J.:Poradnik Inżyniera Spawalnictwo,tom II. Wydawnictwa NaukowoTechniczne. Warszawa 2005.



Agata Wieczorska and Rafał Domzalski

- [4] Grigorenko G. M., Kostin W. A.:Spawalność stali i kryteria jej oceny. Przegląd Spawalnictwa 7/2013.
- [5] Zadroga L.: Technologia spawania oraz jej kwalifikowanie dla stali konstrukcyjnych z uwzględnieniem właściwości złączy spawanych.
- [6] Główne niezgodności spawalnicze. FIGEL. Opracowanie Kemppi Sp. z o.o. https://figel.pl/wiedza/technologia-spawania/glowne-niezgodnościspawalnicze-oraz-metody-ich-zapobiegania/ (dostęp 01.12.2021)
- [7] Sędek P.: Jakość technologii spawania. Instytut Spawalnictwa, Gliwice. Przegląd budowlany 1/2009.
- [8] Spawanie łukiem krytym SAW. http://www.e-spawalnik.pl/?spawanie-lukiemkrytym-saw,106 (dostęp 01.12.2021)
- [9] Charakterystyka spawania łukiem krytym (saw)https://spawalnicy.pl/edukacja/57-charakterystyka-spawania-lukiemkrytym-saw (dostęp 01.12.2021)